Biosafety and Health 8 (2026) 63–70

Contents lists available at ScienceDirect

Biosafety and Health

journal homepage: www.elsevier.com/locate/bsheal

Original Research

A semi-mechanistic modeling strategy for infectious diseases forecasting: Error correction and probabilistic prediction

Zihan Hao [a], Jiaxuan Hu [a], Shujuan Hu [a,b,*], Zhen Zhang [a], Donghuai Jia [a], Jianping Huang [a,b,*]

[a] College of Atmospheric Sciences, Lanzhou University, Lanzhou 730000, China
[b] Collaborative Innovation Center for Western Ecological Safety, College of Atmospheric Sciences, Lanzhou University, Lanzhou 730000, China

ARTICLE INFO

Article history:
Received 29 June 2025
Revised 16 December 2025
Accepted 17 December 2025
Available online 18 December 2025

Keywords:
Infectious disease modeling
Prediction error
Error correction
Probabilistic prediction

ABSTRACT

Global climate change and technological advancements have intensified the threats of pandemics, while complex transmission dynamics challenge infectious disease forecasting. Traditional compartmental models struggle to fully capture both the dynamic transmission processes and their associated uncertainties. Here, we develop a novel hybrid methodology that integrates dynamic modeling with statistical approaches, establishing a semi-mechanistic model for error correction and probabilistic prediction. Our error analysis of the dynamic model reveals that frequent population mobility compromises the accuracy of dynamic predictions and that meteorological conditions further modulate forecast performance by regulating human movement patterns. To capture these effects, we implement a quantile regression long short-term memory (QRLSTM) network to estimate prediction errors of the epidemic dynamic model based on mobility and environmental data. This hybrid approach corrects dynamic prediction errors and generates probabilistic forecasts. Validation using multi-state the United States (U.S.) coronavirus disease 2019 (COVID-19) outbreak data shows that our framework reduces dynamic prediction errors by over 50 %. Compared with pure deep learning approaches, the semi-mechanistic model significantly enhances long-term prediction performance and interpretability. By integrating mechanistic modeling with data-driven learning, the proposed approach improves the predictive accuracy and reliability of models in real-world outbreaks, thereby delivering more effective decision support for public health interventions.

1. Introduction

In the field of public health, infectious disease forecasting has long been a critical research priority, playing a vital role in safeguarding human health and promoting socioeconomic stability. Currently, the acceleration of global climate change has created more favorable environments for the survival of certain viruses, whereas rapid technological advancements have diversified and facilitated human travel patterns [1–3]. These developments accelerate the transmission of infectious diseases and escalate public health risks, while also increasing the complexity of transmission dynamics. Consequently, current strategies for modeling infectious diseases face more severe challenges.

Compartmental models [e.g., susceptible-infected-recovered (SIR), susceptible-exposed-infected-recovered (SEIR)] have long served as classical tools for modeling infectious disease dynamics [4]. These models categorize the population into distinct compartments based on health status (e.g., susceptible, infected, recovered) and describe the temporal evolution of each subgroup using systems of differential equations. Compartmental models effectively illustrate the transmission mechanisms of infectious diseases and enable the evaluation of various intervention strategies [5]. However, traditional compartmental models exhibit certain limitations in practical applications [6,7], particularly in capturing the numerous uncertain influencing factors and complex transmission dynamics inherent in real-world epidemics [8–10]. In response, researchers often enhance model complexity by introducing additional compartments and time-varying transmission parameters [5,11–13]. While this improves the characterization of complex epidemic dynamics, the resulting complexity exacerbates practical challenges, especially in estimating initial conditions and parameters [14]. Therefore, data assimilation techniques, such as the Kalman filter and Ensemble Kalman Filter, have been introduced to reduce the uncertainty in the initial conditions and parameters of infectious disease dynamic models [15,16], enabling real-time estimation of parameters and system states [17–19]. In addition, to explicitly incorporate uncertainty, a common and fundamental approach is to extend deterministic models into the framework of stochastic differential equations (SDEs). SDEs have been widely adopted to model the

* Corresponding authors: College of Atmospheric Sciences, Lanzhou University, Lanzhou 730000, China (S. Hu and J. Huang).
E-mail addresses: hushuju@lzu.edu.cn (S. Hu), hjp@lzu.edu.cn (J. Huang).

https://doi.org/10.1016/j.bsheal.2025.12.002
2590-0536/

HIGHLIGHTS

Scientific questions

Infectious disease forecasting faces increasingly complex challenges due to climate change and technological advancements, which heighten viral transmission risks and complicate disease spread dynamics. A key challenge lies in developing infectious disease modeling that balances mechanistic interpretability with data-driven flexibility to improve forecast accuracy and quantify uncertainty.

Evidence before this study

Current infectious disease modeling employs two paradigms: mechanistic and data-driven models. Compartmental models, which are classical tools for modeling infectious disease dynamics, excel in theoretical interpretability but cannot precisely handle real-world uncertainties and complex transmission dynamics. Deep learning can capture complex patterns from heterogeneous data but provides limited epidemiological insight. However, the restricted interpretability of current deep learning approaches regarding transmission mechanisms limits their application in mechanistic analysis.

New findings

Our semi-mechanistic infectious diseases forecasting framework significantly enhances long-term prediction capability while maintaining a certain degree of model interpretability. By extracting latent signals from extensive meteorological and population mobility datasets, the model supplements conventional surveillance data with critical transmission dynamics signatures while quantifying outbreak uncertainty. These advances improve prediction accuracy by over 50 %. In addition, our study shows that population mobility and meteorological factors significantly affect susceptible-exposed-infectious-recov ered-dead (SEIRD) model prediction errors. Frequent travel complicates the transmission of infectious diseases and brings more uncertainty, making it difficult for traditional dynamic prediction models to accurately forecast epidemics.

Significance of the study

The semi-mechanistic infectious diseases forecasting framework preserves mechanistic interpretability while utilizing deep learning to capture complex mobility-weather-disease interactions, enabling more accurate and actionable epidemic forecasts.

inherent randomness in epidemic dynamics, such as for influenza and coronavirus disease 2019 (COVID-19), providing a rigorous mathematical foundation for analyzing disease extinction and persistence [20–22].

In parallel, the rapid advancement of deep learning has introduced novel modeling techniques for epidemic prediction [23–26]. These data-driven deep learning models can efficiently process large volumes of epidemic-related data (e.g., environmental, population mobility data) and identify latent patterns. However, the limited interpretability of current deep learning approaches regarding transmission mechanisms hinders their utility for mechanistic analysis. Therefore, developing hybrid modeling frameworks that integrate domain knowledge of disease dynamics while capturing complex real-world epidemic patterns and associated uncertainties poses a pivotal challenge in contemporary infectious disease forecasting research.

In this study, we propose a semi-mechanistic hybrid modeling framework that uses a deep learning network to revise errors in the compartmental model and enable the probabilistic prediction of the cumulative number of infections. Since it is impossible to build a perfect model through a “process correction” approach, this approach aims to enhance all dimensions of the model and optimize the parameters [27]. We considered an alternative approach to model error correction: a posteriori correction, achieved by estimating and integrating prediction errors from the dynamic model into the final forecasts. Thus, we decompose disease transmission into two components: (1) a deterministic component with clear dynamics; and (2) an uncertain component reflecting unknown dynamics. Firstly, we employ the classical susceptible-exposed-infectious-recovered-dead (SEIRD) compartmental model to represent the deterministic transmission mechanism, which captures the baseline transmission mechanism. Then, leveraging rich datasets on meteorological and population mobility, we apply quantile regression long short-term memory (QRLSTM) to account for the residual dynamics not captured by the mechanistic model, correcting prediction errors of the compartmental model while generating probabilistic forecasts that quantify uncertainty in transmission. This semi-mechanistic framework integrates the interpretability of mechanistic models with the powerful pattern recognition capabilities of data-driven approaches, offering a more comprehensive basis for public health decision-making.

2. Materials and methods

2.1. Research data

The datasets used in this study are summarized in Table 1. Daily cumulative confirmed COVID-19 cases for each U.S. state are sourced from the COVID-19 dataset maintained by the Center for Systems Science and Engineering at Johns Hopkins University (Fig. S1) (https://github.com/CSSEGISandData/COVID-19). To reduce data noise, a 7-day moving average was applied to cumulative cases for each state. Furthermore, we obtained daily new cases by applying first-order differencing to cumulative case numbers. To identify epidemic periods, we defined the outbreak onset as the first day with a non-zero increase in confirmed cases, and the end of the outbreak as the point when daily new cases returned to zero. Based on this criterion, we selected 49 COVID-19 outbreaks in the continental U. S., each lasting at least 100 days (Table S1).

Daily meteorological data were sourced from the Fifth Generation European Centre for Medium-Range Weather Forecasts Atmospheric Reanalysis of the Global Climate (ERA5) reanalysis dataset (https://cds.climate.copernicus.eu), including minimum temperature (T_{min}), maximum temperature (T_{max}), mean temperature (T_{mean}), relative humidity (RH), mean wind speed (W_{mean}), and total precipitation (TP), with a spatial resolution of 0.25° × 0.25°. Population mobility data comprise daily population not staying at home ($POP_{not\ home}$)and the number of trips across varying distances ($Trips_i$, i is the distance range of trip) within each U.S. state. These data, obtained from the daily travel dataset provided by the U.S. Bureau of Transportation Statistics (https://www.bts.gov/covid-19), reflect the potential impact of population movement on the spread of the epidemic during the public health emergency.

2.2. Error correction and probabilistic forecasting framework

The semi-mechanistic epidemic forecasting framework we developed (SEIRD-QRLSTM) is illustrated in Fig. 1. The process starts by using a conventional SEIRD model to describe epidemic transmission

Table 1
The data used in the study.

Variables	Label	Description	Unit
COVID-19 data	C_{cum}	Daily cumulative number of confirmed cases	persons
	I_{new}	Daily new cases	persons
Meteorological data	T_{min}	Daily minimum temperature	℃
	T_{max}	Daily maximum temperature	℃
	T_{mean}	Daily mean temperature	℃
	RH	Daily relative humidity	%
	W_{mean}	Daily mean wind speed	m/s
	TP	Daily total precipitation	mm
Population mobility data	$POP_{not\ home}$	Daily population not staying at home	persons
	$Trips_{<1\ km}$	Daily number of trips less than 1 km	numbers
	$Trips_{1-3\ km}$	Daily number of trips within 1 to 3 km	numbers
	$Trips_{3-5\ km}$	Daily number of trips within 3 to 5 km	numbers
	$Trips_{5-10\ km}$	Daily number of trips within 5 to 10 km	numbers
	$Trips_{10-25\ km}$	Daily number of trips within 10 to 25 km	numbers
	$Trips_{25-50\ km}$	Daily number of trips within 25 to 50 km	numbers
	$Trips_{50-100\ km}$	Daily number of trips within 50 to 100 km	numbers
	$Trips_{100-250\ km}$	Daily number of trips within 100 to 250 km	numbers
	$Trips_{250-500\ km}$	Daily number of trips within 250 to 500 km	numbers
	$Trips_{\geqslant 500\ km}$	Daily number of trips over 500 km	numbers

Abbreviation: COVID-19, coronavirus disease 2019.

dynamics. Using observed epidemic data, the model parameters are calibrated through least-squares estimation to produce an optimal dynamic forecast. The residuals between the dynamic forecast and actual observations, which represent the prediction errors, subsequently serve as the target for the QRLSTM network. By integrating multiple source data, such as meteorological factors, human mobility records, historical epidemic observations, and dynamic prediction data, the QRLSTM model estimates the prediction errors. Finally, the predicted errors are incorporated back into the dynamic forecasts. This integration achieves error correction for the dynamic predictions while simultaneously generating probabilistic forecasts.

2.2.1. SEIRD model

The SEIRD model divides the population into five compartments: susceptible (S), exposed (E), infected (I), recovered (R), and dead (D). It is assumed that within a specific region, the total population N consists of the five aforementioned groups ($N = S + E + I + R + D$). Susceptible individuals may become exposed upon contact with either infectious or exposed individuals. Exposed individuals have a certain probability of progressing to the infectious stage. During the course of infection, infectious individuals may either recover or die, transitioning into the R or D compartments, respectively. The model is governed by a set of nonlinear ordinary differential equations parameterized by five key parameters: the transmission rate (β), which determines the likelihood of infection upon contact; the incubation rate (α), representing the rate at which exposed individuals become infectious; the relative infectiousness of exposed individuals compared to infectious individuals (θ); the recovery rate (γ); and the mortality rate (μ), reflecting the probabilities of recovery and death, respectively. Furthermore, since our dataset comprised daily cumulative number of confirmed cases, we incorporated an auxiliary compart-

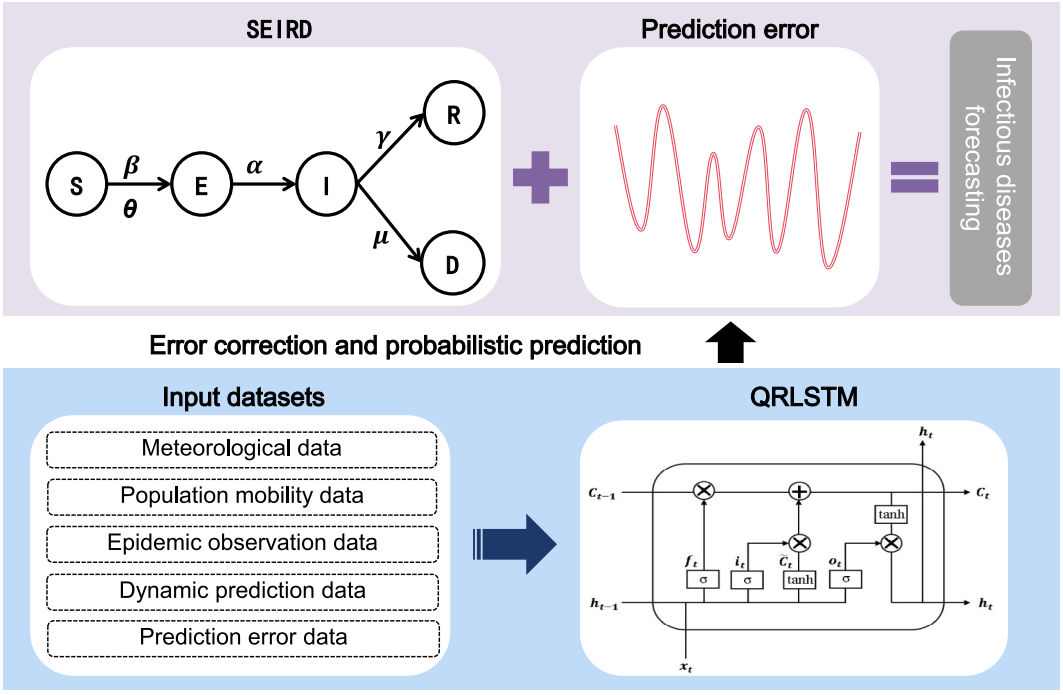

Fig. 1. The framework for error correction and probabilistic prediction of infectious diseases. The purple background area represents the SEIRD dynamic forecast and its prediction errors, while the blue area denotes the QRLSTM-based error prediction module. The final prediction is obtained by combining the errors predicted by the QRLSTM model with the dynamic forecast. Abbreviations: SEIRD, susceptible (S) – exposed (E) – infectious (I) – recovered (R) – dead (D); QRLSTM, quantile regression long short-term memory.

ment tracking cumulative confirmed cases (A) within the SEIRD structure. This adaptation ensures alignment between model states and observational data, which facilitates the use of the model.

$$\begin{cases} \frac{dS}{dt} = -\frac{\beta S(I+\theta E)}{N}, \\ \frac{dE}{dt} = \frac{\beta S(I+\theta E)}{N} - \alpha E, \\ \frac{dI}{dt} = \alpha E - \gamma I - \mu I, \\ \frac{dR}{dt} = \gamma I, \\ \frac{dD}{dt} = \mu I, \\ \frac{dA}{dt} = \alpha E. \end{cases} \tag{1}$$

2.2.2. QRLSTM model

The QRLSTM is a deep learning method that combines the temporal modeling capabilities of long short-term memory networks (LSTM) with the probabilistic forecasting strength of quantile regression [28–30]. LSTM alleviates the issues of gradient disappearance and gradient explosion in recurrent neural networks (RNN), enabling the network to learn long-term dependencies within the data, making it particularly suitable for analyzing and predicting time series data [28] (Supplementary Data). In our study, the LSTM network learns long-term dependencies from historical meteorology, population mobility, epidemic observations, and dynamic prediction residuals. We employ quantile loss functions in place of mean squared error to train the model to predict specific quantiles (5^{th}, 50^{th}, and 95^{th} percentiles), thus producing prediction intervals rather than single-point estimates. The quantile loss function for quantile $q \in \{0.05,\ 0.5,\ 0.95\}$ is defined as:

$$L_q(y,\hat{y}) = \begin{cases} q(y-\hat{y}) & if\ y \geqslant \hat{y}, \\ (1-q)(y-\hat{y}) & if\ y < \hat{y}, \end{cases} \tag{2}$$

where $\hat{y}_i$ is the predicted result and y_i is the observed value. This asymmetric loss penalizes overestimation and underestimation differently, guiding the model to learn specific quantile behaviors. By utilizing a multi-output architecture, QRLSTM can provide valuable uncertainty quantification through the 0.05 and 0.95 quantiles, spanning a 90% confidence interval around the median forecast. Unlike traditional regression models that estimate only the conditional mean of the target variable, QRLSTM directly estimates conditional quantiles, allowing for the prediction of a range of possible future values and capturing uncertainty in time series forecasting.

2.3. Experimental setup

First, we applied a seven-day moving average to reduce noise in the epidemic observation data. For each U.S. state, an initial set of SEIRD model states was generated, and the optimal parameters were estimated using the least squares method (Supplementary Data). Based on these estimates, dynamic predictions of daily new cases were computed for each U.S. state. Furthermore, the differences between the dynamic predictions and the observed daily new cases were calculated and defined as the dynamic prediction errors. These errors were used as the target variable for the QRLSTM model, while the input features included meteorological conditions, population mobility, observed daily new cases and dynamic prediction errors over the previous 12 days (the lag order is obtained based on the autocorrelation analysis of the dynamic prediction errors shown in Fig. S2). Finally, the different quantiles ($q \in \{0.05,\ 0.5,\ 0.95\}$) of dynamic prediction errors predicted by the QRLSTM model were added to the dynamic predictions to obtain the error-corrected daily new cases.

we compared the prediction results before and after error correction using multiple evaluation metrics. In addition, under the same experimental conditions, we compared the QRLSTM-based error correction with LSTM-based error correction, as well as direct epidemic prediction using deep learning models (QRLSTM and LSTM). The experiments employed five-fold cross-validation, in which 80 % of the data (39 states) were randomly assigned to the training set and 20 % (10 states) to the test set in each fold. All input features underwent min–max normalization (Eq. (3), with test sets exclusively using training set extreme values to prevent data leakage.

$$x_{\text{norm}} = \frac{x - x_{\text{min}}^{\text{train}}}{x_{\text{max}}^{\text{train}} - x_{\text{min}}^{\text{train}}}, \tag{3}$$

where x_{min}^{train} and x_{max}^{train} denotes the minimum and maximum values of the train data, respectively. Detailed parameter settings for each model in the comparative experiments are provided in Supplementary Data.

To validate the accuracy of error correction and probabilistic forecasting, this study employs the root mean square error (RMSE) and symmetric mean absolute percentage error (SMAPE) to evaluate model performance. RMSE is a widely used metric to measure the differences between predicted values and observed values. For predictions $\hat{y}_i$ and observations y_i with n samples, RMSE is defined as:

$$RMSE = \sqrt{\frac{1}{n}\sum_{i=1}^{n}(\hat{y}_i - y_i)^2} \tag{4}$$

SMAPE is symmetric and normalizes the absolute error by the average of the absolute predicted and observed values, which prevents the error from being disproportionately large when observed values are close to zero. This makes SMAPE more robust and reliable, especially in datasets where values may approach or reach zero, providing a balanced and interpretable measure of relative forecasting accuracy. SMAPE is defined as:

$$SMAPE = \frac{1}{n}\sum_{i=1}^{n}\frac{|\hat{y}_i - y_i|}{(|y_i| + |\hat{y}_i|)/2} \tag{5}$$

3. Results

3.1. Population mobility and meteorological factors complicate epidemic predictions

Identifying the factors influencing prediction errors in the SEIRD model is crucial for its error correction. Using the Mantel test, we analyzed the impact of meteorological conditions and population mobility on dynamic prediction errors. In our analysis, we used the absolute values of dynamic prediction errors. The results indicate that population mobility significantly influences dynamic model prediction errors (Fig. 2A). Travel activities at different distances exhibit varying degrees of correlation with dynamic prediction errors. Short-distance travel has a more pronounced impact on local epidemic forecasts than long-distance travel. Frequent travel activities complicate the transmission process of infectious diseases and introduce greater uncertainty, making it difficult for traditional dynamic prediction models to accurately forecast epidemics. Additionally, meteorological factors exhibit a weaker direct relationship with dynamic prediction errors than population mobility does. Only wind speed exhibits a certain degree of correlation with dynamic prediction errors.

In contrast to the direct correlation observed between population mobility and dynamic prediction errors, meteorological factors demonstrate a comparatively weaker association. Only wind speed demonstrated a certain degree of correlation with dynamic prediction errors. However, meteorological factors have been shown to significantly contribute to population mobility (Fig. 2B). Therefore, meteoro-

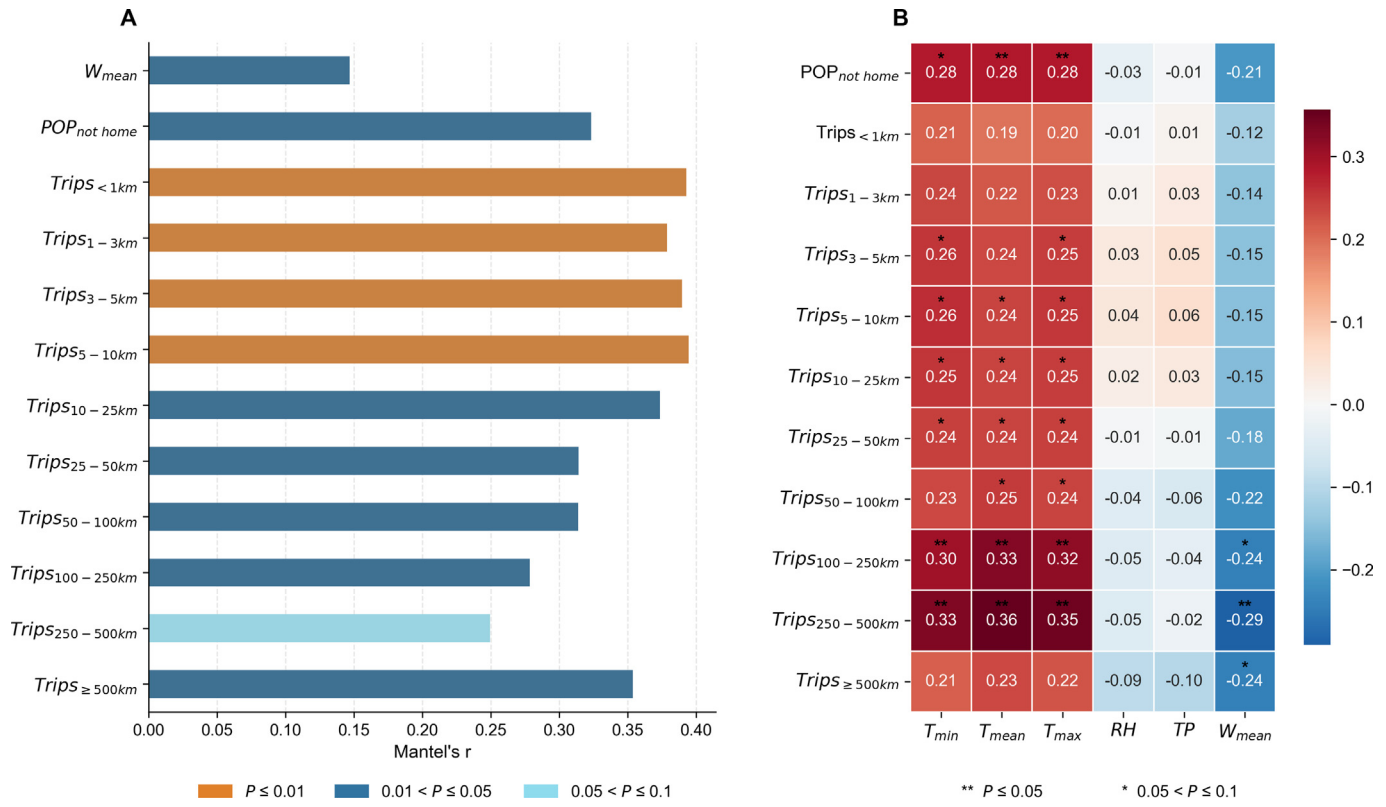

Fig. 2. Analysis of the factors that influence dynamic prediction error. A) Mantel test results for the influence of meteorological and population mobility factors on dynamic prediction errors. Only the results that passed the significance test are shown in the figure. B) Pearson correlation coefficient between meteorological factors and population mobility. ** $P < 0.05$, * $P < 0.1$. Abbreviations: T_{min}, minimum temperature; T_{max}, maximum temperature; T_{mean}, mean temperature; RH, relative humidity; W_{mean}, mean wind speed; TP, total precipitation; $POP_{not\text{-}home}$, daily population not staying at home; $Trips_i$, the number of trips across varying distances, i is the distance range of trip.

logical conditions can affect the spread of epidemics by altering people's travel patterns. In subsequent deep learning modeling for error correction, we incorporated meteorological factors and population mobility data as model inputs. This approach enables extraction of richer epidemiological insights, compensating for gaps in the dynamic model's representation of transmission dynamics.

3.2. Error correction reduces the epidemic dynamics prediction error

Comparative analysis reveals substantially reduced prediction errors in testing datasets across multiple forecast days (1, 3, and 7 days) following error correction (Fig. 3). On average, the relative error (SMAPE) of the 7-day-ahead corrected predictions decreased by over 50 % compared to the original SEIRD dynamic model outputs. These results validate the effectiveness of our error revision process.

More importantly, the incorporation of error correction markedly enhances the ability to capture rapid changes in epidemic dynamics and enhances the accuracy of peak-day predictions. Fig. 4 illustrates the probabilistic forecasting performance for Texas and Louisiana. The median trajectory of predicted cumulative infection cases shows close alignment with actual observations, successfully capturing epidemic rebounds. In addition, the probabilistic output provides valuable uncertainty quantification through 0.05 and 0.95 quantiles, visualized as a 90 % confidence interval around the central forecast. Furthermore, we compare prediction errors for the epidemic peak day before and after error correction. The results demonstrate that with a 7-day ahead correction, the average peak-day error rate decreases from 40 % to 10 %, while the average deviation in peak timing is reduced to within 10 days.

3.3. Advantages of the semi-mechanistic model in long-term prediction

The baseline predictions from the dynamical forecasting model provide epidemiological principle-based constraints for the error correction model, ensuring that prediction errors do not grow indefinitely. The integration of the dynamical model with deep learning error correction enhances the accuracy of long-term epidemic forecasts. Fig. 5 compares the prediction performance of the semi-mechanistic model and the black-box model (pure deep learning model) across different forecasting horizons. Within approximately two weeks, the semi-mechanistic model achieves prediction errors comparable to those of the pure deep learning model (Fig. 5). However, for forecasts extending beyond two weeks, the prediction errors of the semi-mechanistic model are significantly smaller (Fig. 5). While data-driven deep learning models possess strong data-fitting capabilities, achieving accurate long-term predictions has remained a persistent challenge. The semi-mechanistic model demonstrates stronger generalization capability and practical utility. The hybrid forecasting framework that combines dynamical and statistical methods represents an effective modeling approach for obtaining both long-term predictive accuracy and interpretability in epidemic forecasting.

4. Discussion

The semi-mechanistic epidemic forecasting framework developed in this study dynamically refines mechanistic model projections using deep learning, building upon baseline infection predictions and transmission parameters. This framework significantly lowers the barrier to

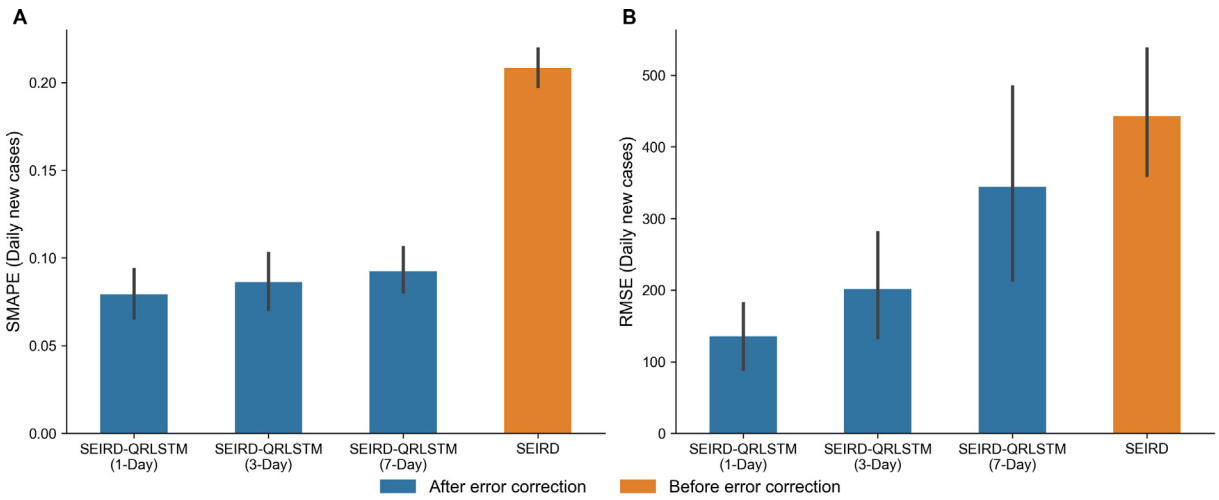

Fig. 3. Comparison of daily new case prediction errors before and after error correction. The average results from 49 states after error revisions are shown in blue, compared with the average predictions of the original SEIRD model in orange. The black line represents the 95 % confidence interval. A) Comparison of the SMAPE before and after error correction (including error correction for different lead periods: 1 day, 3 days, and 7 days). B) Comparison of the RMSE before and after error correction (including error correction for different lead periods: 1 day, 3 days, and 7 days). Abbreviations: SEIRD, susceptible-exposed-infectious-recovered-dead; QRLSTM, quantile regression long short-term memory; SMAPE, symmetric mean absolute percentage error; RMSE, root mean square error.

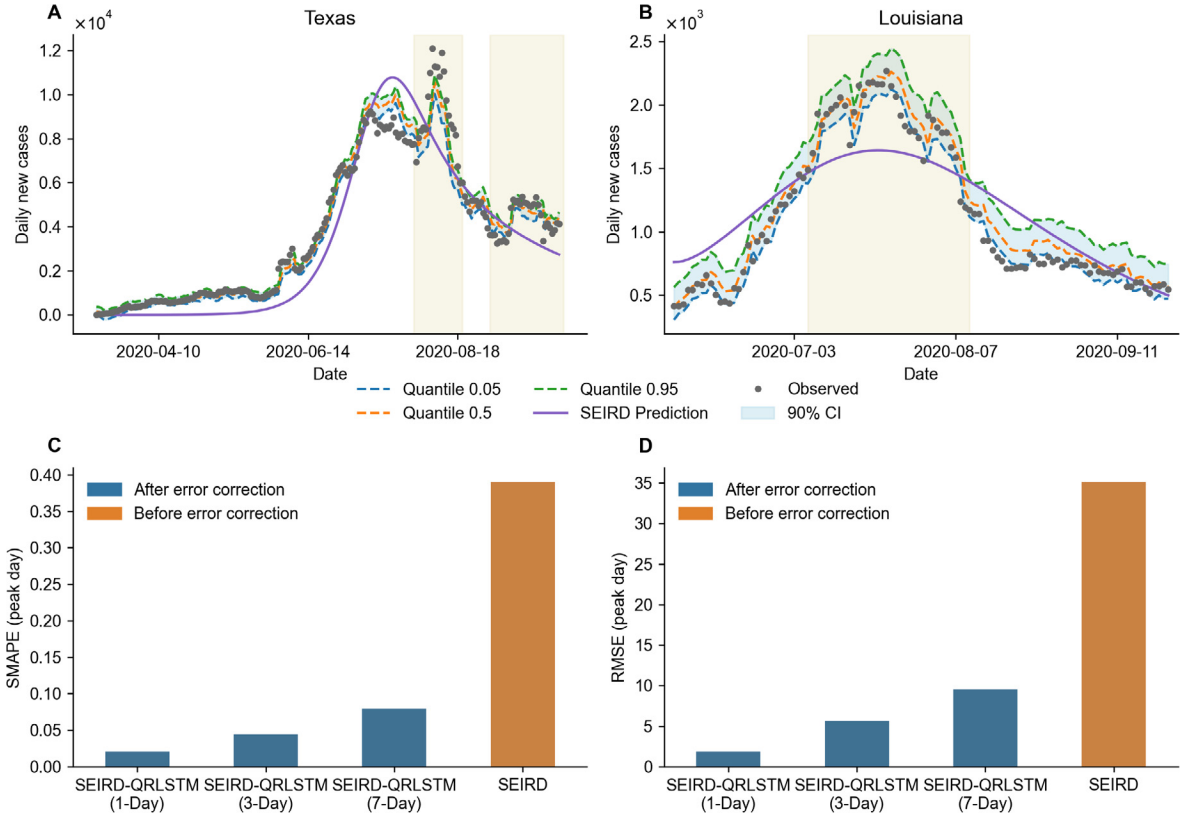

Fig. 4. Probabilistic forecasting performance and peak-day error analysis. A) Daily new cases in Texas predicted by the SEIRD-QRLSTM model compared with the baseline SEIRD model. The gray points are the observed values. The purple line is the dynamic prediction result. The orange dotted line represents the median of the probability prediction by the SEIRD-QRLSTM model. The green dotted line represents the 0.95 percentile of the probability prediction, and the blue dotted line represents the 0.05 percentile of the probability prediction. The blue band between the 0.05 and 0.95 quantiles represents the 90% confidence interval (CI). B) Same as (A), but for Louisiana. C) SMAPE of peak-day predictions before and after error correction. D) RMSE of peak-day predictions before and after error correction. Abbreviations: SEIRD, susceptible-exposed-infectious-recovered-dead; QRLSTM, quantile regression long short-term memory; SMAPE, symmetric mean absolute percentage error; RMSE, root mean square error.

implementing epidemiological dynamic models. Even when transmission mechanisms are not fully understood, it enables reasonably accurate predictions using a simple SEIRD model. It significantly enhances long-term prediction capability while maintaining a certain degree of model interpretability. By extracting latent signals from extensive meteorological and population mobility datasets, the model supple-

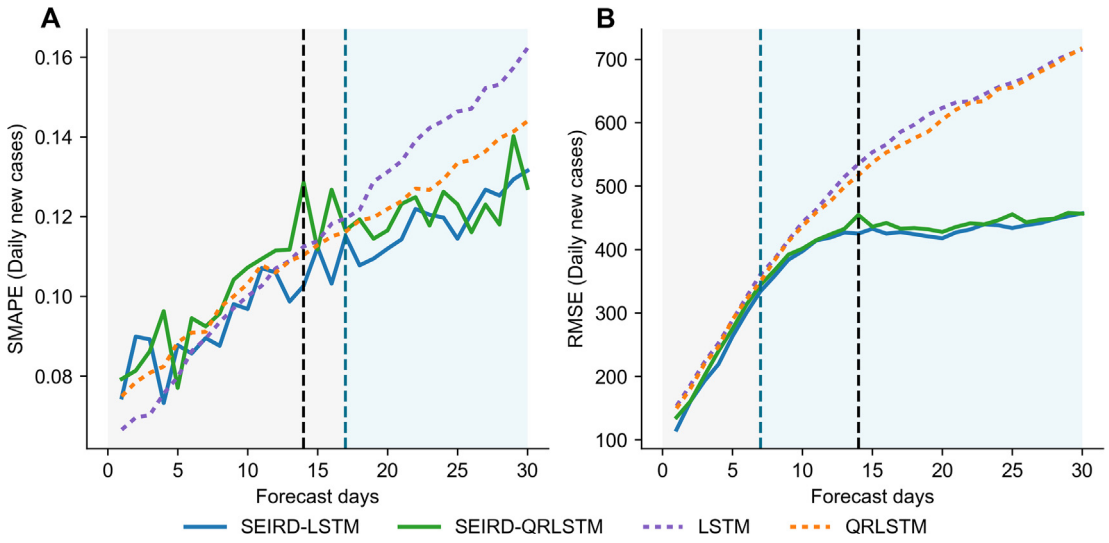

Fig. 5. Comparison of the prediction effect of the semi-mechanistic model and the black-box model at different prediction durations. The blue solid line represents the SEIRD-LSTM model, the green solid line represents the SEIRD-QRLSTM model, the purple dotted line represents the LSTM model, and the yellow dotted line represents the QRLSTM model. A) SMAPE of daily new cases for multiple models with different prediction durations. B) RMSE of daily new cases for multiple models with different prediction durations. Abbreviations: SEIRD, susceptible-exposed-infectious-recovered-dead; QRLSTM, quantile regression long short-term memory; SMAPE, symmetric mean absolute percentage error; RMSE, root mean square error; LSTM, long short-term memory.

ments conventional surveillance data with critical transmission dynamics signatures while quantifying outbreak uncertainty. These advances improve prediction accuracy by over 50 % and directly inform public health interventions such as mobility restriction strategies.

Despite effectively integrating mechanistic and statistical modeling paradigms, several limitations warrant acknowledgment. Our error correction methodology was validated solely on a basic SEIRD model that did not incorporate time-varying transmission parameters, limiting its capacity to represent complex dynamic behaviors. Future research should integrate more sophisticated mechanistic formulations while implementing dynamic parameter error correction. Furthermore, the framework cannot entirely eliminate prediction errors stemming from initial value inaccuracies. Subsequent work will incorporate data assimilation techniques to holistically optimize three error dimensions: initial conditions, parameter estimation, and model structural uncertainty.

In summary, the rapid and increasingly complex spread of the pandemic has intensified the demand for infectious disease prediction modeling strategies. Traditional dynamical models encounter challenges in achieving precise epidemic forecasts. Our analysis indicates a significant correlation between population mobility and prediction errors in dynamical models. High-frequency population movement increases the complexity of human contact, thereby increasing errors in infectious disease dynamical predictions. Meteorological factors further complicate these predictions by influencing travel activities. To tackle these limitations, this study incorporates meteorological factors and population mobility to conduct error correction research on the conventional dynamical prediction model SEIRD. We have ultimately developed a semi-mechanistic infectious disease prediction strategy that merges dynamical modeling with statistical approaches. This framework utilizes deep learning models to correct errors in traditional dynamical forecasts and enables probabilistic forecasting of cumulative infection cases. Tested across U.S. states during the COVID-19 pandemic, our corrected cumulative case predictions showed significant improvement over uncorrected results, validating the framework's effectiveness. Furthermore, our approach quantifies prediction uncertainty. The error-correction and probabilistic forecasting framework enhances the practical utility of traditional dynamical models while compensating for their inherent limitations in characterizing transmission mechanisms and uncertainties.

Acknowledgements

This study was supported by the National Key Research and Development Program of China (2023YFC3503400), R&D Program of Guangzhou Laboratory (SRPG22-007), Major Project of Guangzhou National Laboratory (GZNL2024A01004).

Conflict of interest statement

The authors declare that there are no conflicts of interest.

Author Contributions

Zihan Hao: Writing – review & editing, Writing – original draft, Visualization, Validation, Software, Methodology, Data curation. **Jiaxuan Hu:** Writing – review & editing, Visualization, Data curation. **Shujuan Hu:** Writing – review & editing, Supervision, Resources, Funding acquisition, Conceptualization. **Zhen Zhang:** Writing – review & editing, Visualization, Data curation. **Donghuai Jia:** Writing – review & editing. **Jianping Huang:** Writing – review & editing, Supervision, Project administration, Funding acquisition, Conceptualization.

Supplementary data

Supplementary data to this article can be found online at https://doi.org/10.1016/j.bsheal.2025.12.002.

References

[1] C.J. Carlson, G.F. Albery, C. Merow, C.H. Trisos, C.M. Zipfel, E.A. Eskew, K.J. Olival, N. Ross, S. Bansal, Climate change increases cross-species viral transmission risk, Nature 607 (2022) 555–562, https://doi.org/10.1038/s41586-022-04788-w.

[2] A. Findlater, I.I. Bogoch, Human mobility and the global spread of infectious diseases: A focus on air travel, Trends Parasitol. 34 (2018) 772–783, https://doi.org/10.1016/j.pt.2018.07.004.
[3] M.N. Lessani, Z. Li, F. Jing, S. Qiao, J. Zhang, B. Olatosi, X. Li, Human mobility and the infectious disease transmission: A systematic review, Geo. Spat. Inf. Sci. 27 (6) (2024) 1824–1851, https://doi.org/10.1080/10095020.2023.2275619.
[4] W.O. Kermack, A.G. McKendrick, G.T. Walker, A contribution to the mathematical theory of epidemics, Proc. R. Soc. Lond. A 115 (1927) 700–721, https://doi.org/10.1098/rspa.1927.0118.
[5] B. Tang, X. Wang, Q. Li, N.L. Bragazzi, S. Tang, Y. Xiao, J. Wu, Estimation of the transmission risk of the 2019-nCoV and its implication for public health interventions, J. Clin. Med. 9 (2020) 462, https://doi.org/10.3390/jcm9020462.
[6] S. Funk, S. Bansal, C.T. Bauch, K.T.D. Eames, W.J. Edmunds, A.P. Galvani, P. Klepac, Nine challenges in incorporating the dynamics of behaviour in infectious diseases models, Epidemics 10 (2015) 21–25, https://doi.org/10.1016/j.epidem.2014.09.005.
[7] W.C. Roda, M.B. Varughese, D. Han, M.Y. Li, Why is it difficult to accurately predict the COVID-19 epidemic?, Infect Dis. Model. 5 (2020) 271–281, https://doi.org/10.1016/j.idm.2020.03.001.
[8] H.S. Badr, H. Du, M. Marshall, E. Dong, M.M. Squire, L.M. Gardner, Association between mobility patterns and COVID-19 transmission in the USA: A mathematical modelling study, Lancet Infect. Dis. 20 (2020) 1247–1254, https://doi.org/10.1016/S1473-3099(20)30553-3.
[9] J.D. Ford, C. Zavaleta-Cortijo, T. Ainembabazi, C. Anza-Ramirez, I. Arotoma-Rojas, J. Bezerra, V. Chicmana-Zapata, E.K. Galappaththi, M. Hangula, C. Kazaana, et al., Interactions between climate and COVID-19, Lancet Planet. Health 6 (2022) e825–e833, https://doi.org/10.1016/S2542-5196(22)00174-7.
[10] X. Lian, J. Huang, H. Li, Y. He, Z. Ouyang, S. Fu, Y. Zhao, D. Wang, R. Wang, X. Guan, Heat waves accelerate the spread of infectious diseases, Environ. Res. 231 (2023) 116090, https://doi.org/10.1016/j.envres.2023.116090.
[11] O.N. Bjørnstad, K. Shea, M. Krzywinski, N. Altman, The SEIRS model for infectious disease dynamics, Nat. Methods 17 (2020) 557–558, https://doi.org/10.1038/s41592-020-0856-2.
[12] Y. Chen, P. Lu, C. Chang, T. Liu, A time-dependent SIR model for COVID-19 with undetectable infected persons, IEEE Trans. Netw. Sci. Eng. 7 (2020) 3279–3294, https://doi.org/10.1109/TNSE.2020.3024723.
[13] J. Huang, L. Zhang, X. Liu, Y. Wei, C. Liu, X. Lian, Z. Huang, J. Chou, X. Liu, X. Li, et al., Global prediction system for COVID-19 pandemic, Sci. Bull. 65 (2020) 1884–1887, https://doi.org/10.1016/j.scib.2020.08.002.
[14] O. Melikechi, A.L. Young, T. Tang, T. Bowman, D. Dunson, J. Johndrow, Limits of epidemic prediction using SIR models, J. Math. Biol. 85 (2022) 36, https://doi.org/10.1007/s00285-022-01804-5.
[15] A. Schaum, R. Bernal-Jaquez, L. Alarcon Ramos, Data-assimilation and state estimation for contact-based spreading processes using the ensemble kalman filter: Application to COVID-19, Chaos, Solitons Fractals 157 (2022) 111887, https://doi.org/10.1016/j.chaos.2022.111887.
[16] S. Rosa, M.A. Pulido, J.J. Ruiz, T.J. Cocucci, Transmission matrix parameter estimation of COVID-19 evolution with age compartments using ensemble-based data assimilation, PLoS One 20 (2025) e0318426, https://doi.org/10.1371/journal.pone.0318426.
[17] J. Song, H. Xie, B. Gao, Y. Zhong, C. Gu, K.S. Choi, Maximum likelihood-based extended Kalman filter for COVID-19 prediction, Chaos, Solitons Fractals 146 (2021) 110922, https://doi.org/10.1016/j.chaos.2021.110922.
[18] X. Zhu, Y. Shi, Y. Zhong, An EKF prediction of COVID-19 propagation under vaccinations and viral variants, Math. Comput. Simul. 231 (2025) 221–238, https://doi.org/10.1016/j.matcom.2024.12.012.
[19] Y. Shi, X. Zhu, X. Zhu, B. Cheng, Y. Zhong, Kalman filter-based epidemiological model for post-COVID-19 Era surveillance and prediction, Sensors 25 (2025) 2507, https://doi.org/10.3390/s25082507.
[20] B. Boukanjime, T. Caraballo, M. El Fatini, M. El Khalifi, Dynamics of a stochastic coronavirus (COVID-19) epidemic model with Markovian switching, Chaos, Solitons Fractals 141 (2020) 110361, https://doi.org/10.1016/j.chaos.2020.110361.
[21] X. Zhu, B. Gao, Y. Zhong, C. Gu, K.S. Choi, Extended Kalman filter based on stochastic epidemiological model for COVID-19 modelling, Comput. Biol. Med. 137 (2021) 104810, https://doi.org/10.1016/j.compbiomed.2021.104810.
[22] K.M. Mohammad, Md. Kamrujjaman, Stochastic differential equations to model influenza transmission with continuous and discrete-time Markov chains, Alex. Eng. J. 110 (2025) 329–345, https://doi.org/10.1016/j.aej.2024.10.012.
[23] M.O. Alassafi, M. Jarrah, R. Alotaibi, Time series predicting of COVID-19 based on deep learning, Neurocomputing 468 (2022) 335–344, https://doi.org/10.1016/j.neucom.2021.10.035.
[24] M.R. Davahli, K. Fiok, W. Karwowski, A.M. Aljuaid, R. Taiar, Predicting the dynamics of the COVID-19 pandemic in the united states using graph theory-based neural networks, IJERPH 18 (2021) 3834, https://doi.org/10.3390/ijerph18073834.
[25] F. Shahid, A. Zameer, M. Muneeb, Predictions for COVID-19 with deep learning models of LSTM, GRU and Bi-LSTM, Chaos, Solitons Fractals 140 (2020) 110212, https://doi.org/10.1016/j.chaos.2020.110212.
[26] L. Zhou, C. Zhao, N. Liu, X. Yao, Z. Cheng, Improved LSTM-based deep learning model for COVID-19 prediction using optimized approach, Eng. Appl. Artif. Intell. 122 (2023) 106157, https://doi.org/10.1016/j.engappai.2023.106157.
[27] H. Ren, J. Chou, Study progress in prediction strategy and methodology on numerical model, Adv. Earth Sci. 22 (4) (2007) 376–385, https://doi.org/10.3321/j.issn:1001-8166.2007.04.007.
[28] S. Hochreiter, J. Schmidhuber, Long short-term memory, Neural Comput. 9 (1997) 1735–1780, https://doi.org/10.1162/neco.1997.9.8.1735.
[29] R. Koenker, K.F. Hallock, Quantile Regression, J. Econ. Perspect. 15 (2001) 143–156, https://doi.org/10.1257/jep.15.4.143.
[30] Z. Zhang, H. Qin, Y. Liu, L. Yao, X. Yu, J. Lu, Z. Jiang, Z. Feng, Wind speed forecasting based on quantile regression minimal gated memory network and kernel density estimation, Energy Conv. Manag. 196 (2019) 1395–1409, https://doi.org/10.1016/j.enconman.2019.06.024.